European Radiology (2019) 29:429–438
https://doi.org/10.1007/s00330-018-5398-y

ONCOLOGY

Gliosarcoma: a clinical and radiological analysis of 48 cases

Xiaoping Yi[1,2] · Hang Cao[3] · Haiyun Tang[1] · Guanghui Gong[4] · Zhongliang Hu[4] · Weihua Liao[1] · Lunquan Sun[2,5] · Bihong T. Chen[6] · Xuejun Li[3]

Received: 21 December 2017 / Revised: 15 February 2018 / Accepted: 21 February 2018 / Published online: 12 June 2018

Abstract

Objectives To retrospectively review the radiological and clinicopathological features of gliosarcoma (GSM) and differentiate it from glioblastoma multiforme (GBM).

Methods The clinicopathological data and imaging findings (including VASARI analysis) of 48 surgically and pathologically confirmed GSM patients (group 1) were reviewed in detail, and were compared with that of other glioblastoma (GBM) cases in our hospital (group 2).

Results There were 28 men and 20 women GSM patients with a median age of 52.5 years (range, 24-80 years) in this study. Haemorrhage ($n = 21$), a salt-and-pepper sign on T2-weighted images ($n = 36$), unevenly thickened wall ($n = 36$) even appearing as a paliform pattern ($n = 32$), an intra-tumoural large feeding artery ($n = 32$) and an eccentric cystic portion (ECP) ($n = 19$) were more commonly observed in the GSM group than in GBM patients. Based on our experience, GSM can be divided into four subtypes according to magnetic resonance imaging (MRI) features. When compared to GBM (group 2), there were more patients designated with type III lesions (having very unevenly thickened walls) and IV (solid) lesions among the GSM cases (group 1). On univariate prognostic analysis, adjuvant therapy (radiotherapy, chemotherapy, and radiochemotherapy) and existence of an eccentric cyst region were prognostic factors. However, Cox's regression model showed only adjuvant therapy as a prognostic factor for GSM.

Conclusions When compared to GBM, certain imaging features are more likely to occur in GSM, which may help raise the possibility of this disease. All GSM patients are recommended to receive adjuvant therapy to achieve a better prognosis with radiotherapy, chemotherapy or radiochemotherapy all as options.

Key Points

- *Diagnosis of gliosarcoma can be suggested preoperatively by imaging.*
- *Gliosarcoma can be divided into four subtypes based on MRI.*
- *Paliform pattern and ECP tend to present in gliosarcoma more than GBM.*
- *The cystic subtype of gliosarcoma may predict a more dismal prognosis.*
- *All gliosarcoma patients should receive adjuvant therapy to achieve better prognosis.*

Xiaoping Yi and Hang Cao contributed equally to this work.

Electronic supplementary material The online version of this article (https://doi.org/10.1007/s00330-018-5398-y) contains supplementary material, which is available to authorized users.

✉ Xuejun Li
lxjneuro@csu.edu.cn

[1] Department of Radiology, Xiangya Hospital, Central South University, No. 87 Xiangya Road, Changsha, Hunan 410008, People's Republic of China

[2] Postdoctoral Research Workstation of Pathology and Pathophysiology, Basic Medical Sciences, Xiangya Hospital, Central South University, No. 87 Xiangya Road, Changsha, Hunan 410008, People's Republic of China

[3] Department of Neurosurgery, Xiangya Hospital, Central South University, No. 87 Xiangya Road, Changsha, Hunan 410008, People's Republic of China

[4] Department of Pathology, Xiangya Hospital, Central South University, No. 87 Xiangya Road, Changsha, Hunan 410008, People's Republic of China

[5] Center for Molecular Medicine, Xiangya Hospital, Central South University, No. 87 Xiangya Road, Changsha, Hunan 410008, People's Republic of China

[6] Department of Diagnostic Radiology, City of Hope National Medical Center, Duarte, CA, USA

Keywords Gliosarcoma · Glioblastoma · Magnetic resonance imaging · Multidetector computed tomography · Prognosis

Abbreviations

ECP	Eccentric cystic portion
GBM	Glioblastoma multiforme
GSM	Gliosarcoma
HGG	High-grade glioma
IHC	Immunohistochemical
OS	Overall survival
PSM	Propensity score matching
VASARI	Visually accessible rembrandt images

Introduction

Gliosarcoma (GSM) is a rare central nervous system (CNS) tumour, which has been reported to have similar clinical and radiological presentation to glioblastoma multiforme (GBM) and an even poorer prognosis [1–7]. Given the inadequate knowledge of this rare disease, no specific or special therapy is yet available for GSM. GBM guidelines remain the only available treatment strategy regardless of the poorer prognosis for GSM compared with GBM [8]. It has been noted that a different treatment strategy or new potential clinical therapy is strongly needed for GSM in order to achieve a longer survival [1, 2, 4, 5, 9, 10]. Thus, an accurate preoperative diagnosis may be mandatory prior to the attempt to develop optimal treatment strategies in the clinic [4, 5, 11]. However, preoperative needle biopsy remains the only reliable method to obtain accurate preoperative diagnosis of this obscure brain tumour to date. Unfortunately, diagnosis based on puncture biopsy still has a high probability of misdiagnosis, not to mention its invasive nature and inherent medical risks, such as accidental implantation of tumour tissue along the puncture canal. In addition, whether biopsy diagnosis is accurate or not depends on the suitability of the sample, as well as on the diagnostic pathologist's awareness of the disease. All of these reasons together limit the clinical application of biopsy. For example, when referring to patients with suspected high-grade glioma (HGG), biopsy should be alternative only if GSM is considered likely. Therefore, non-invasive radiological examination, especially magnetic resonance imaging (MRI), which could provide reliable diagnostic clues or potentially achieve an accurate diagnosis preoperatively, has always been a hot issue in this field [12–14].

Considering the rarity of this disease, only a few studies with limited data have previously focused on GSM [1–5, 8, 11, 15–20]. Among these, the majority focus on clinicopathological data, and specific radiological studies are seriously lacking. Given the few imaging features of this rare tumour that have been demonstrated, GSM is still poorly recognised radiologically. Clinically, GSM is easily misdiagnosed as GBM preoperatively due to its extremely low incidence and similar radiological presentation [6, 19, 21]. Thus, it is challenging for radiologists and surgeons to make a reasonably accurate preoperative diagnosis of GSM, even when aware of this rare disease. A comprehensive study of GSM radiological features with significant diagnostic value as well as their underlying pathological basis is therefore urgently needed.

Herein, we report a retrospective study of 48 patients with surgically and pathologically proven GSM at our hospital. The primary purpose was to identify the radiological findings (focusing on MRI) of this rare disease and their diagnostic value for differentiating it from GBM. The treatment and prognosis factors of this disease are also discussed.

Materials and methods

Design and patients

This retrospective study was approved by our hospital's institutional review board (no. 201709995), and the requirement for informed consent was waived.

From January 2008 to April 2017, all patients with surgically and pathologically confirmed GBM or GSM were searched in our hospital's medical record database. A flowchart of the patients enrolled for analysis, along with numbers of excluded patients and the reasons for their exclusion, is shown in Fig. 1.

MR and CT imaging analysis

MR and CT images were regularly obtained in our hospital (details shown in supplementary files). Two radiologists (H.T., W.L.) specialising in nervous system diseases (with more than 6 and 15 years' experience, respectively) independently evaluated the CT and MRI features of the imaging data, including the size, shape, margin, haemorrhage, intra-tumoural feeding artery and patterns of appearance, CT attenuation/MRI intensity, and enhancement patterns. For all tumours with MRI images, a Visually Accessible Rembrandt Images (VASARI) analysis was performed. Each lesion was scored according to the VASARI as previously described, with 30 imaging features being evaluated. Among these 30 features, 27 were ultimately used, while three (F26, 27, 28) were excluded due to the lack of postoperational MRI in some patients. A complete description of the VASARI feature set can be found on the internet (https://wiki.nci.nih.gov/display/CIP/VASARI) [22]. The investigators were all blinded to the histopathological results, and inconsistencies were resolved via consensus.

In the present study, all cases with MRI images were classified as one of four subtypes, I, II, III, or IV, mainly based on the degree of uneven thickening of the tumour wall on enhanced images A cystic mass with mild-to-moderately thickened wall was defined as subtype I. If the thickened wall was

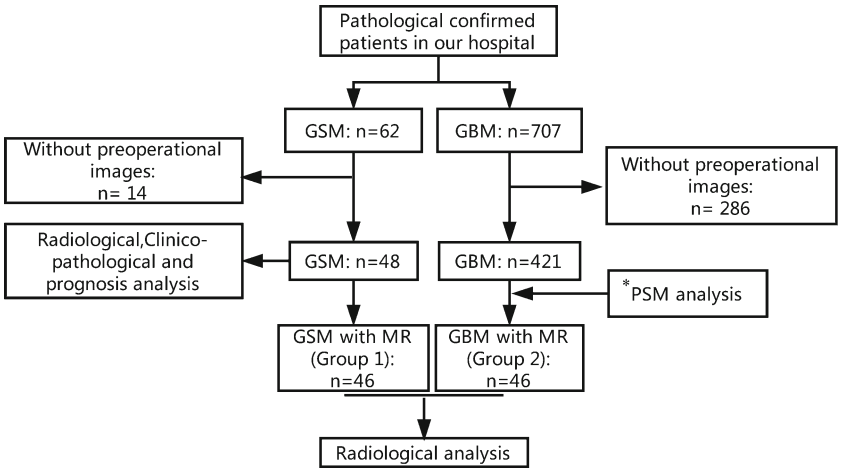

Fig. 1 Flowchart of the present study. *PSM propensity score matching

intermediate or marked, accompanied by an inner wall that was becoming uneven, a subtype II or III was assigned. When the tumour was all solid, it was classified as subtype IV (a more detailed depiction can be found in the supplementary files). Based on the overall impression of the mass after reviewing all the images, we carried out the typing by using quantitative criteria based on the proportion of the total area of the tumour that showed a solid structure. The criteria were defined as follows: subtype I, <35%; II, 35-64%; III, 65-94%; IV, ≥95%.

In addition, each subtype was further divided into two groups, depending upon whether or not there were accompanying cystic portions (marked with the subscript letter C). A pattern map of the subtypes described above and representative images of corresponding cases are shown in Fig. 2.

The inter-reader agreement for the main radiological features was evaluated using the kappa consistency test. Excellent, good and poor agreement were defined as kappa values of >0.81, in the range of 0.61–0.80 and <0.60, respectively.

The pathological sections of all enrolled GSM patients, including the haematoxylin and eosin (H&E) and immunohistochemical (IHC) staining, were reanalysed independently by two experienced pathologists (Z.H., G.G.). The findings were recorded by consensus.

Follow-up

The follow-up period was determined as from the first day of diagnosis to the day of death or the date of the last follow-up examination.

Statistics

Statistics and propensity score matching (PSM) analysis were performed using SPSS 22.0 (IBM, Armonk, NY, USA). For the quantitative features, the Wilcoxon rank-sum test was used. For the qualitative features, chi-squared test or Fisher's exact test were used to test differences between groups. Statistical analysis of survival was performed using the Kaplan-Meier method, and the results were examined using the log-rank test. Cox multivariate survival analyses was also performed. A p value less than 0.05 was considered statistically significant.

Results

Clinical data

According to the study design, 48 consecutive patients (group 1) with pathologically proven GSM were enrolled in this study, and 46 gender- and age-matched GBM cases were selected as the control group (group 2) as shown in Fig. 1.

The 28 men and 20 women of group 1 in this study had a median age of 52.5 years (range, 24–80 years). The clinical symptoms that contributed to the diagnosis were diverse and non-specific (Table 1). All of the GSM patients were preoperatively misdiagnosed as having other types of tumours, including meningioma (n = 3), GBM (n = 16), or a vague diagnosis of high-grade glioma (n = 29). There were no significant differences between group 1 and group 2 with respect to demographic data ($p > 0.05$). Details can be found in Supplementary Table S1.

Inter-reader agreement

Inter-reader analysis showed good-to-excellent agreement in main imaging features including VASARI scores (kappa value = 0.687–1.000) (Supplementary Table S2).

Imaging findings

The main imaging findings for the 48 GSM cases are shown in Table 1 and Supplementary Table S3. Most of the masses in our study showed a peripheral location (45/48, 93.8%) and tendency to invasion of the dura (24/46, 52.2%) or ependymal layer (17/46, 37.0%).

Generally, GSM appeared predominantly as low-attenuation masses, with a mean CT value of 15-28 HU on the CT images.

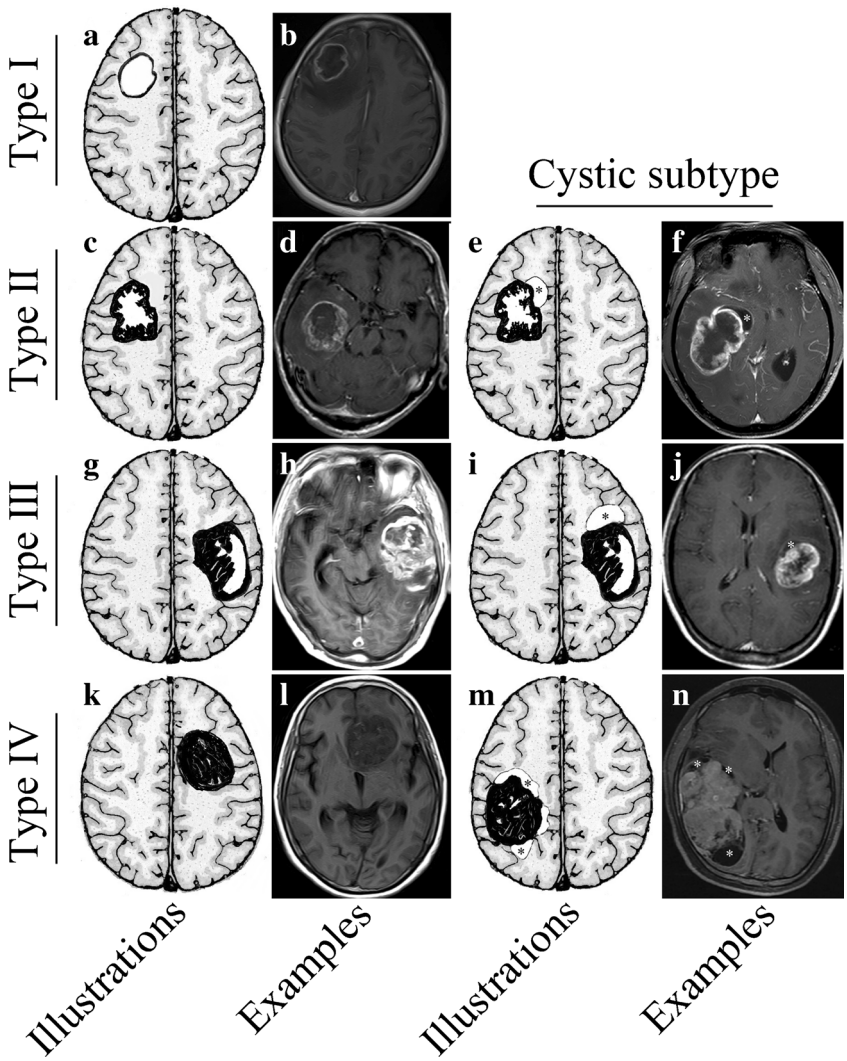

Fig. 2 Illustration and typical examples the four imaging subtype patterns of GSM, including subtype I (**a**, **b**), II (**c**, **d**), II_c (**e**, **f**), III (**g**, **h**), III_c (**i**, **j**), IV (**k**, **l**), IV_c (**m**, **n**). The eccentric cysts of "$_c$" subtype GSM are clearly demonstrated by *asterisks* (**e**, **f**, **i**, **j**, **m**, **n**)

On MRI images, most of the legions appeared as well demarcated masses with a heterogeneous appearance, appearing heterogeneously iso- to hypo-intense on the T1-weighted images, and mixed hypo-/homo-/hyper-intense on the T2-weighted images. Unevenly thickened walls with a strong rim- and a ring-like or paliform enhancement (P-E) patterns could be observed in 36 (78.26%) of 46 GSM patients with MRI images. Haemorrhage at different stages, which resulted in a salt-and-pepper (S-P) sign on T2- or T1-weighted images, could be observed in 67.39% (31/46) of cases (Fig. 3 and Supplementary Fig. S1).

Regarding the subtypes, type I ($n = 2$) (Fig. 1), type II ($n = 18$) (including II_c, $n = 7$), type III ($n = 16$) (including III_c, $n = 9$) (Fig. 1) and type IV ($n = 10$) (including IV_c, $n = 3$) (Fig. 1) all could be detected in group 1. When compared to GBM (group 2), there are more patients designated with type III and IV lesions among the GSM cases (group 1), consistent with the imaging findings mentioned above. Interestingly, a higher proportion of cystic subtypes was observed in group 1.

In addition, masses with mild or moderate enhancement pattern and some interesting findings were also observed in GSM patients. For instance, aneurysmal-like enhanced nodules were found in three GSM cases with type IV masses, including one case appearing with a mild enhancement pattern (Supplementary Fig. S2).

There are some apparent differences between GSM and GBM on images. For GBM cases, all the features depicted above, especially the S-P sign and unevenly thickened walls with strong rim/ring-like or P-E pattern, can also be observed. However, the degree of thickening of the wall in GSM tends to be more obvious, accompanied by a higher rate of haemorrhage, the presence of an eccentric cystic region and a P-E pattern (Supplementary Table S4).

Subsequent χ^2 tests confirmed the association with GSM cases (group 1) of the features mentioned above, including P-E pattern, advanced subtype, ECP, S-P sign and also with several VASARI features (F5-8, 15, 16, 17, 19, 20, 29, 30). The differences in imaging features between group 1 and

Table 1 Clinical data of 48 GSM cases

Characteristic	Number of patients (n = 48)	
Chief complaint		
Headache	31	65
Vomit	13	29
Nausea	4	9
Numbness	9	19
Unstable gait	4	9
Age		
Average age, years	53.9	
Median age, years	52.5	
Sex		
Male	28	62
Female	20	38
KPS		
90	9	19
80	29	60
70	10	21
Tumour location		
Frontal	8	17
Temporal	13	27
Parietal	1	2
Occipital	1	2
Ventricle	5	10
Cerebellum	1	2
Brain stem	0	2
Overlapping/NOS	19	40
Resection		
Extended	7	19
Gross total	37	60
Subtotal/unknown	4	22
Radiotherapy	16	15
Chemotherapy	16	30

group 2 are shown in a heat-map (Fig. 4). Details are shown in Supplementary Tables S4 and S5.

Treatment and pathological findings

Surgery was performed in all patients, and adjuvant radiotherapy, chemotherapy, or radiochemotherapy were recommended to all patients according to the guidelines for treatment of GBM. Details can be found in Supplementary Table S1.

Pathological typing was evaluated in surgical specimens. Generally, GSM lesions were irregular (n = 32) or oval/lobulated (n = 16) masses with a grey or yellowish-white appearance, and demonstrated a biphasic tissue pattern that was composed of a mixture of gliomatous and sarcomatous tissues as demonstrated previously [20]. The stain for GFAP clearly distinguished true gliosarcoma portions (positive) from sarcomatous components (negative) (Fig. 5). A large number of bleeding foci and abundant blood vessels could be found in the tumours, which may explain the appearance of imaging signs such as the S-P sign and the P-E pattern.

Generally, the lesions had a relatively high Ki-67 index ranging from 10 to 80% in IHC analysis. Most noteworthy, lesions identified as a cystic subtype were seen to have a higher Ki-67 index than non-cystic lesions (52 ± 17% vs 31 ± 20%), though the difference was not significant ($p > 0.05$). A small proportion of patients were positive for MGMT (12/36, 33.3%). Positive staining for IDH1 was rare (2/32, 6.25%).

The histopathological findings combined with IHC stains confirmed the identification of GSM. Details are displayed in Supplementary Table S1.

Follow-up

Three patients (cases 5, 8 and 18) were lost to follow-up. Another two patients (cases 2 and 34) were lost during follow-up without any known medical reasons. The remaining 43 patients received follow-up after discharge. The median follow-up time was 10 months (range, 3-46 months). Median overall survival (OS) for all patients was 12.0±1.9 (range, 3-46) months after diagnosis.

Univariate prognostic analysis demonstrated that GSM patients undergoing adjuvant therapy achieved a significantly better prognosis, with the median OS (18.0 ± 1.3 months) significantly higher than for patients who declined any adjuvant therapy (9.0 ± 1.5 months) ($p < 0.05$). The patient with cystic subtype was also linked to a worse prognosis, with a significantly lower median OS (10.0 ± 2.5 months vs 19.0 ± 6.0 months) ($p < 0.05$) (Fig. 6).

Cox's multifactorial regression model showed only adjuvant therapy as a significant prognostic factor for GSM (Supplementary Table S2). The cystic subtype did not achieve a significant effect ($p = 0.13$) (Fig. 6).

Discussion

It has been reported that GSM may demonstrate certain radiological characteristics that could help to differentiate it from GBM [11, 15], including well-demarcated margins, solid-cystic components, the S-P sign, an uneven rim- or ring-like enhancement, as well as intra-tumoural strip enhancement. Unfortunately, all of the highly variable imaging findings of GSM also can be found in other brain malignancies such as GBM and other HGGs, in particular [6]. Significantly, all the patients in this study were misdiagnosed as having either GBM or HGG preoperatively, illustrating the extreme confusion that may occur in clinical practice.

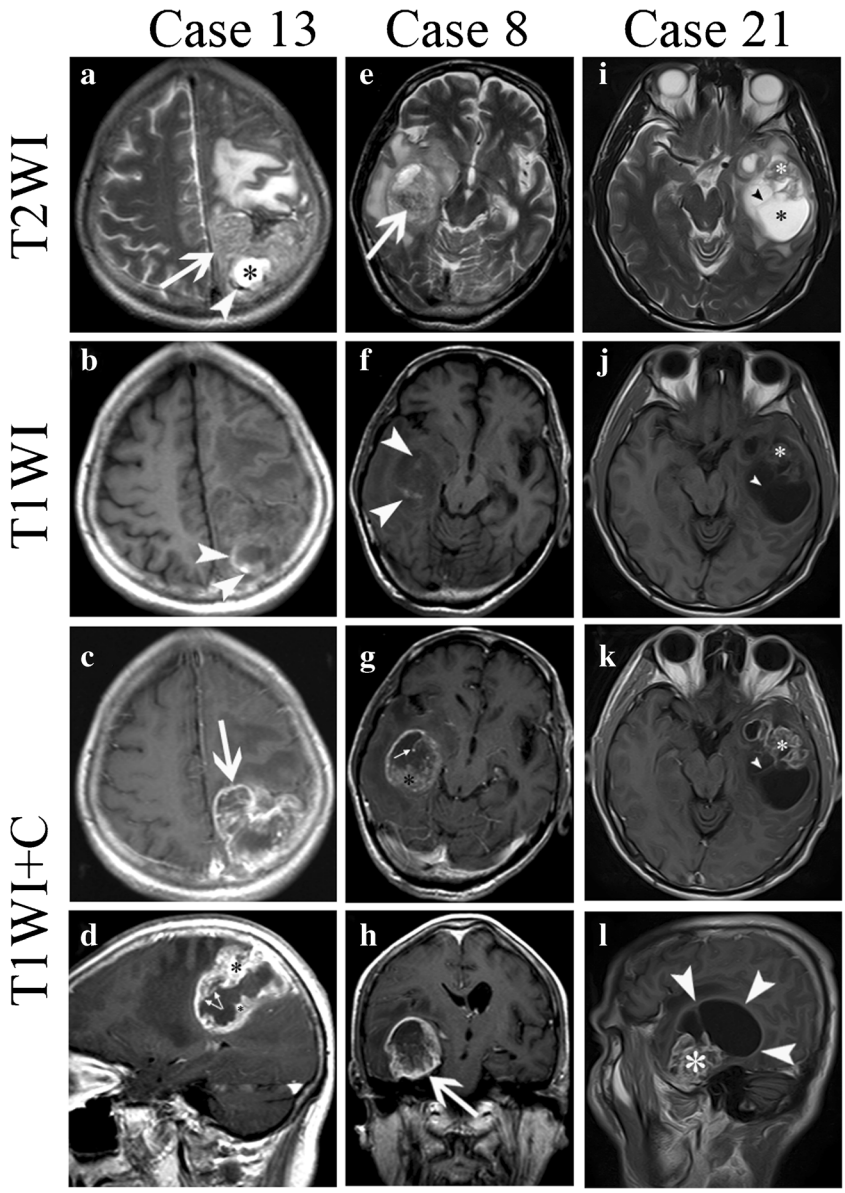

Fig. 3 Case 13 (**a**, **b**, **c**, **d**), a 71-year-old woman with type II lesion. Case 8 (**e**, **f**, **g**, **h**), a 67-year-old man with type II lesion. Case 21 (**i**, **j**, **k**, **l**), a 46-year-old man with type IV_c lesion. In cases 13 and 8, note well-defined masses in left parietal lobe and right temporal lobe showing a salt-and-pepper-like appearance on T2 images (**a**, **e**, *arrow*). In the lesion of case 13, a hyperintense cystic portion (**a**, *asterisk*) was also seen, as well as the posterolateral portion of a cystic structure, corresponding to hypointensity on the T2 image (**a**, *arrowhead*). Note also the abnormal hyperintensity on T1 images (**b**, **f**, *arrowheads*), indicating haemorrhage at subacute phase. On axial (**c**, **g**), sagittal (**d**) and coronal (**h**) enhanced T1 images, abundant intratumoural vessels (a 'comb-like vessel sign') (**c**, **d**, *arrows*) can be clearly seen. Also, markedly enhanced nodules (**d**, **g**, *asterisks*) and intratumoural vessels (**h**, *arrow*) in the unevenly thickened wall are evident. In case 21 (**i**, **j**, **k**, **l**), the lesion in the right temporal lobe appears as a solid-cystic mass, the solid part presenting with low to intermediate signal on T2-weighted imaging (**i**, *white asterisk*) and intermediate signal on T1-weighted imaging (**j**, *asterisk*), while the cystic portion (**i**, *black asterisk*) has high signal on T2-weighted imaging and low signal on T1-weighted imaging. After injection of contrast medium, markedly heterogeneous enhancement is found in the solid portion (**k**, **l**, *asterisk*), while the cystic portion presents with no enhancement except for the cystic wall (**l**, *arrowheads*), resulting in a diamond-ring like appearance (**l**). A slender separation is visible inside the cystic portion (**i**, **j**, *arrowhead*)

In the present study, we retrospectively collected a second biggest GSM cohort in a single centre [21] and try to make a thorough radiological analysis of this rare disease. Moreover, to explore the radiological differences between GSM and GBM more effectively, we constructed a case-matched GBM control group (group 2) by the PSM method, which has never been reported before [6, 8]. Interestingly, though all the named "diagnostic features" depicted above can also be observed in the control GBM cases (group 2), there remain substantial radiological differences between the two groups. Not surprisingly, the statistical comparison results demonstrated that dozens of imaging features in the GSM group,

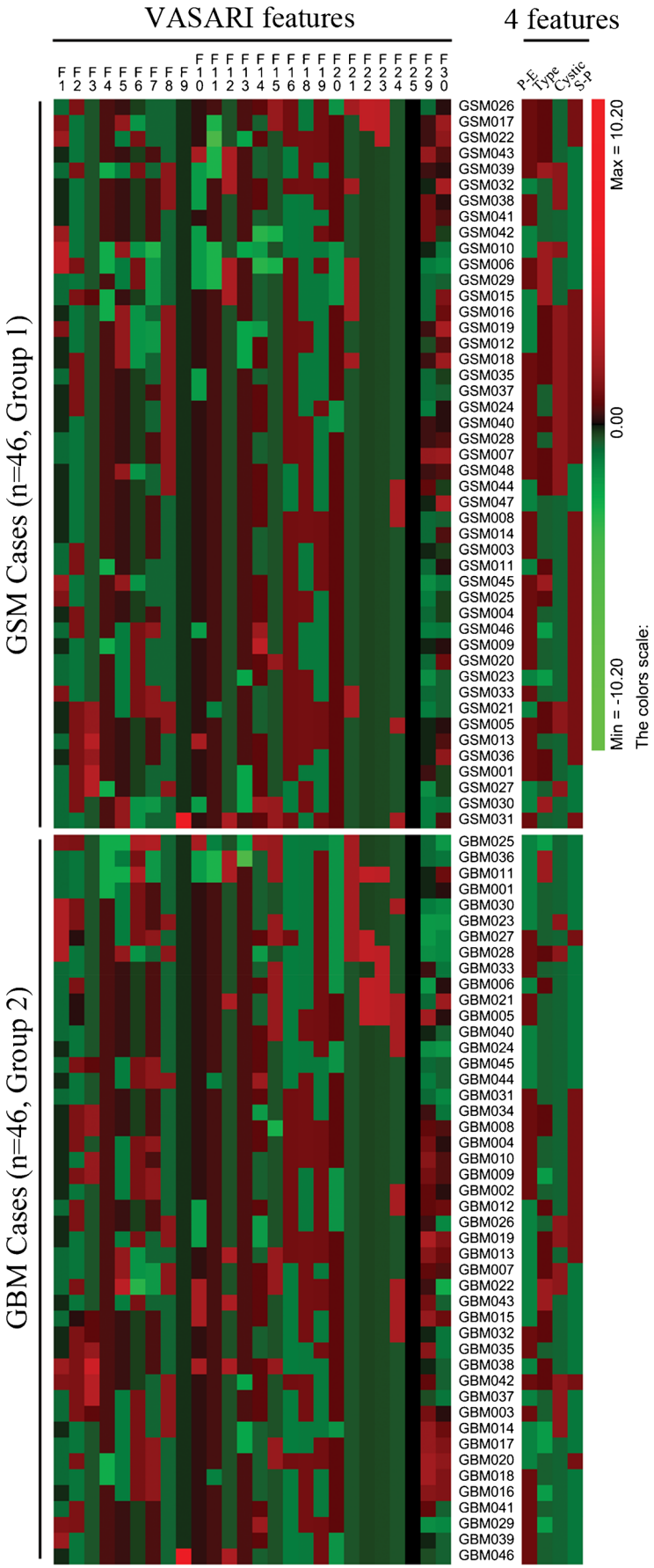

Fig. 4 A heat-map picture demonstrates the difference between VASARI features of GSM cases and GBM cases. *P-E* paliform enhancement, *Type* subtype, *Cystic* eccentric cystic region, *S-P* salt-and-pepper sign

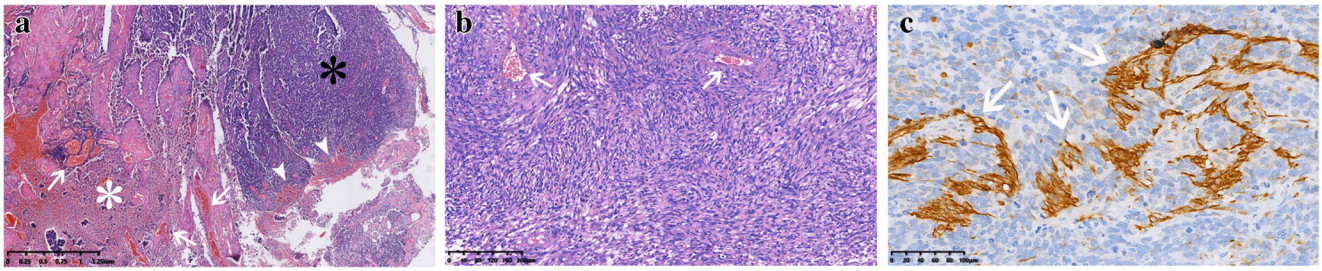

Fig. 5 Pathological findings of GSM. **a** H&E stain shows densely packed bundles of spindle cells (*black asterisk*) with necrosis (*white asterisk*) and haemorrhage (*arrowheads*). Abundant blood vessels can be observed (*arrow*) (40×). **b** The spindle shaped tumour cells were arranged in a fascicular, whorled and storiform pattern, accompanied by blood vessels (*arrow*) (100×). **c** On IHC, the gliomatous component expressing GFAP (*arrows*) intermingled with the GFAP-negative sarcoma component (200×)

including VASARI features, were significantly different from those of GBM cases (see Supplementary Table S3). Generally, the degree of tumour wall thickening tends to be greater in GSM than in GBM, accompanied by a higher rate of haemorrhage and S-P sign, presence of ECP and a P-E pattern.

VASARI analysis also shows some interesting indicators in GSM cases compared to GBM cases which was comparable to previous studies [2, 3, 5, 8, 16, 18, 19, 21, 23, 24]. These indicators confirm that GSM lesions are indeed bigger than GBM lesions, with a higher proportion of enhancement regions (also meaning a lower enhancement ratio), a higher risk of cortical involvement, a lower proportion of necrosis, a lower risk of ependymal invasion and a lower incidence of oedema that crosses the midline. Although preliminary results suggested that the incidence of diffusion-limitation (F17) in GSM was significantly higher than in GBM, the reliability of this feature still needs to be confirmed by further studies because of the small number of patients that underwent diffusion-weighted imaging.

From our experiences in this study, GSM can be classified into four subtypes, I, II, III, and IV, based on the degree of uneven thickening of the tumour wall on enhanced images. There are more patients designated as type III and IV among the GSM cases (group 1) than among the GBM cases (group 2), which was consistent with our initial impressions based on the images from the two groups [16, 21]. Interestingly, a higher proportion of cystic subtype was observed in GSM cases compared to the control group (group 2). Therefore, when a suspicious GBM or HGG tumour with an ECP (especially a III_c case) is encountered in the clinic, the possibility of GSM should be carefully considered.

Traditionally, GSM patients have been treated with GBM-appropriate therapy, and adjuvant radiotherapy is recommended for all GSM patients after surgery [1, 2, 4]. However, the debate over the value of TMZ chemotherapy has still not been resolved due to the lack of a large-scale clinical trial [5, 10, 20, 23]. Our results may plausibly support the argument that chemotherapy added to radiotherapy is ineffective. Interestingly, we found that cystic subtypes, a newly identified imaging feature whose frequency in GSM was significantly higher than in GBM in this study, may have potential for predicting prognosis in GSM patients apart from use in differential diagnosis. GSM patients with a cystic subtype seem to have a more dismal prognosis than other GSM patients, as confirmed in the

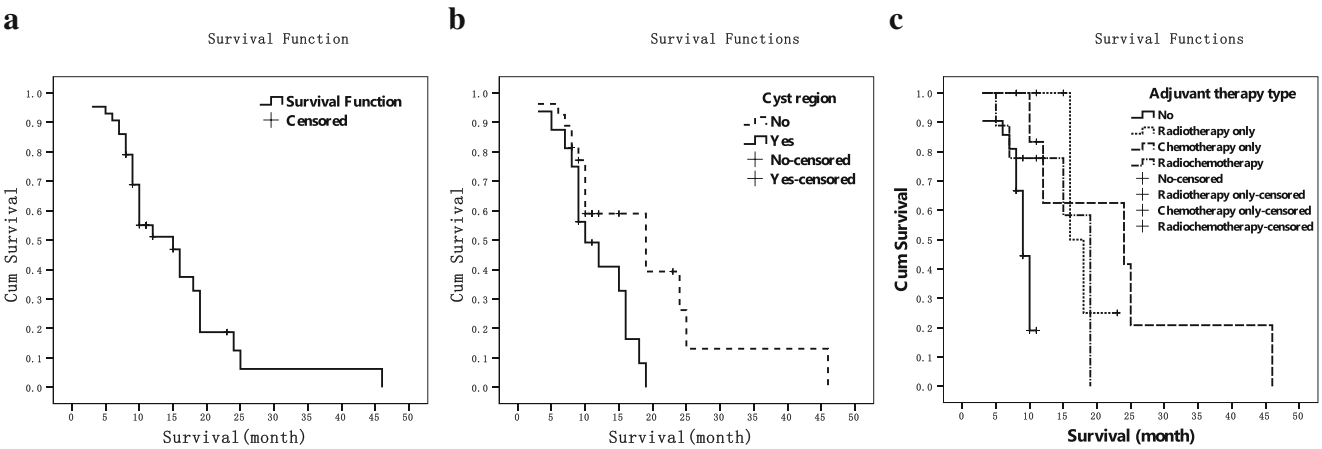

Fig. 6 Kaplan-Meier curve for GSM patients. **a** All GSM patients (n = 45). **b** GSM patients identified as cystic subtype (n = 16) have a poorer prognosis than the non-cystic subtype (n = 27) (p = 0.019). **c** Cox's multifactorial regression model showed that GSM patients receiving adjuvant therapy (radiotherapy, chemotherapy and radiochemotherapy) have a significantly better prognosis than GS patients without any adjuvant therapy after surgery (p = 0.004). There was no difference in prognosis among GSM patients undergoing the different types of adjuvant therapy

univariate prognosis analysis. It is unclear what factors determine whether this feature is present or not. However, the fact that tumours of this subtype have a higher Ki-67 index than tumours without (52 ± 17% vs 31 ± 20%) suggests that the emergence of this feature may be related to the higher growth capacity and more aggressive phenotype of the tumour. Though this impact on prognosis was not significant in the subsequent multivariate analysis, the slightly higher p value ($p = 0.13$) indicates that this may be due to the small number of cases in the present study. Further studies with more cases are needed.

We acknowledge that there are several limitations to the present study. Firstly, the number of cases in this study is small, which may have affected the reliability of the conclusions, although our study is the second largest series in a single institution to our knowledge. Given the rarity of the disease, a small sample size is almost inevitable until a large multi-institutional randomised controlled trial (RCT) can be performed. In addition, the high proportion of patients excluded (14 patients missed preoperative imaging data) may create an inevitable selection bias in the cases enrolled. Second, the long timespan of the enrolled cases and the retrospective nature of this study meant that follow-up of some patients was very difficult, resulting in a relatively high rate of missing and unsatisfactory data. Thirdly, too many patients refused adjuvant therapy or even regular postoperative review after surgery, although we strongly suggested both. Fourthly, the descriptions of diagnostic imaging features identified in our study may depend heavily on the radiologist's personal experience, lack of objective criteria for definitive judgement of such things as the degree of thickening of the tumour wall. A necessary next step will be development of simple, objective, and comparable criteria that will allow radiologists or neurosurgeons to make an accurate judgement. Lastly but significantly, the pathological basis of the imaging findings was not well analysed due to the study's retrospective nature. it is a long way from understanding the biological basis for the diagnostic value of the meaningful features identified in the present study. To approach this, a thorough comparative study on both imaging and pathology needs to be performed prospectively.

Conclusions

Through a case-controlled analysis, we have clearly demonstrated that certain MRI image patterns are more likely to occur in GSM masses than in other GBM cases. The presence of these features may help radiologists and surgeons to be aware of the possibility of a GSM diagnosis preoperatively based on MRI images. Interestingly, a radiologically cystic subtype may be associated with a worse prognosis. Regarding treatment, all GSM patients should be recommended to receive adjuvant therapy to achieve a better prognosis, with radiotherapy, chemotherapy or radiochemotherapy all as valuable options.

Acknowledgements Dr. Xiaoping Yi is right now a Postdoctoral Fellow in Postdoctoral Research Workstation of Pathology and Pathophysiology, Basic Medical Sciences, Xiangya Hospital, Central South University (No. 185705). We thank all the members of Department of Radiology and Professor Li's Lab, Xiangya Hospital, for helpful discussion.

Funding This study has received funding by the National Natural Science Foundation of China (No. 81472594, 81770781)

Compliance with ethical standards

Guarantor The scientific guarantor of this publication is Professor Xuejun Li.

Conflict of interest The authors of this manuscript declare no relationships with any companies, whose products or services may be related to the subject matter of the article.

Statistics and biometry No complex statistical methods were necessary for this paper.

Informed consent Written informed consent was waived by the Institutional Review Board.

Ethical approval Institutional Review Board approval was obtained.

Methodology
- retrospective
- case-control study
- performed at one institution

References

1. Buckner JC, Ballman KV, Michalak JC et al (2006) Phase III trial of carmustine and cisplatin compared with carmustine alone and standard radiation therapy or accelerated radiation therapy in patients with glioblastoma multiforme: North Central Cancer Treatment Group 93-72-52 and Southwest Oncology Group 9503 Trials. J Clin Oncol 24:3871–3879
2. Kozak KR, Mahadevan A, Moody JS (2009) Adult gliosarcoma: epidemiology, natural history, and factors associated with outcome. Neuro Oncol 11:183–191
3. Han SJ, Yang I, Tihan T, Prados MD, Parsa AT (2010) Primary gliosarcoma: key clinical and pathologic distinctions from glioblastoma with implications as a unique oncologic entity. J Neurooncol 96:313–320
4. Walker GV, Gilbert MR, Prabhu SS, Brown PD, McAleer MF (2013) Temozolomide use in adult patients with gliosarcoma: an evolving clinical practice. J Neurooncol 112:83–89
5. Frandsen J, Orton A, Jensen R et al (2017) Patterns of care and outcomes in gliosarcoma: an analysis of the National Cancer Database. J Neurosurg 21:1–6
6. Sampaio L, Linhares P, Fonseca J (2017) Detailed magnetic resonance imaging features of a case series of primary gliosarcoma. Neuroradiol J 30:546–553
7. Louis DN, Perry A, Reifenberger G et al (2016) The 2016 World Health Organization Classification of Tumors of the Central Nervous System: a summary. Acta Neuropathol 131:803–820
8. Damodaran O, van Heerden J, Nowak AK et al (2014) Clinical management and survival outcomes of gliosarcomas in the era of multimodality therapy. J Clin Neurosci 21:478–481

9. Stupp R, Hegi ME, Mason WP et al (2009) Effects of radiotherapy with concomitant and adjuvant temozolomide versus radiotherapy alone on survival in glioblastoma in a randomised phase III study: 5-year analysis of the EORTC-NCIC trial. Lancet Oncol 10:459–466
10. Stupp R, Mason WP, van den Bent MJ et al (2005) Radiotherapy plus concomitant and adjuvant temozolomide for glioblastoma. N Engl J Med 352:987–996
11. Cao H, Wang F, Li XJ (2017) Future strategies on glioma research: from big data to the clinic. Genomics Proteomics Bioinformatics 15:263–265
12. Liao W, Liu Y, Wang X et al (2009) Differentiation of primary central nervous system lymphoma and high-grade glioma with dynamic susceptibility contrast-enhanced perfusion magnetic resonance imaging. Acta Radiol 50:217–225
13. Chang K, Bai HX, Zhou H et al (2017) Residual convolutional neural network for determination of IDH status in low- and high-grade gliomas from MR imaging. Clin Cancer Res 2018, 24(5):1073-1081.
14. Zhou H, Vallières M, Bai HX et al (2017) MRI features predict survival and molecular markers in diffuse lower-grade gliomas. Neuro-Oncology 19:862–870
15. Wanggou S, Feng C, Xie Y, Ye L, Wang F, Li X (2016) Sample level enrichment analysis of KEGG pathways identifies clinically relevant subtypes of glioblastoma. J Cancer 7:1701–1710
16. Singh G, Das KK, Sharma P et al (2015) Cerebral gliosarcoma: analysis of 16 patients and review of literature. Asian J Neurosurg 10:195–202
17. Maiuri F, Stella L, Benvenuti D, Giamundo A, Pettinato G (1990) Cerebral gliosarcomas: correlation of computed tomographic findings, surgical aspect, pathological features, and prognosis. Neurosurgery 26:261–267
18. di Norcia V, Piccirilli M, Giangaspero F, Salvati M (2008) Gliosarcomas in the elderly: analysis of 7 cases and clinicopathological remarks. Tumori 94:493–496
19. Han L, Zhang X, Qiu S et al (2008) Magnetic resonance imaging of primary cerebral gliosarcoma: a report of 15 cases. Acta Radiol 49:1058–1067
20. Meis JM, Martz KL, Nelson JS (1991) Mixed glioblastoma multiforme and sarcoma. A clinicopathologic study of 26 radiation therapy oncology group cases. Cancer 67:2342–2349
21. Zhang BY, Chen H, Geng DY et al (2011) Computed tomography and magnetic resonance features of gliosarcoma: a study of 54 cases. J Comput Assist Tomogr 35:667–673
22. NCBI/NCI/The Cancer Imaging Archive (TCIA) (2016), VASARI (Visually AcceSAble Rembrandt Images) MRI feature set, NCBI/NCI, Bethesda MD. Available via https://wikicancerimagingarchivenet/display/Public/VASARI+Research+Project. Accessed 25 July 2016
23. Machuca TN, Prevedello DM, Pope LZ, Haratz SS, Araújo JC, Torres LF (2004) Gliosarcoma: report of four cases with immunohistochemical findings. Arq Neuropsiquiatr 62:608–612
24. Lutterbach J, Guttenberger R, Pagenstecher A (2001) Gliosarcoma: a clinical study. Radiother Oncol 61:57–64